

# Deep reflection-mode photoacoustic imaging of biological tissue

Kwang Hyun Song and Lihong V. Wang\*

Washington University in St. Louis, Department of Biomedical Engineering, Optical Imaging Laboratory, Campus Box 1097, One Brookings Drive, St. Louis, Missouri 63130-4899

**Abstract.** A reflection-mode photoacoustic (PA) imaging system was designed and built to image deep structures in biological tissues. We chose near-infrared laser pulses of 804-nm wavelength for PA excitation to achieve deep penetration. To minimize unwanted surface signals, we adopted dark-field ring-shaped illumination. This imaging system employing a 5-MHz spherically focused ultrasonic transducer provides penetration up to 38 mm in chicken breast tissue. At the 19-mm depth, the axial resolution is 144  $\mu\text{m}$  and the transverse resolution is 560  $\mu\text{m}$ . Internal organs of small animals were imaged clearly. © 2007 Society of Photo-Optical Instrumentation Engineers. [DOI: 10.1117/1.2818045]

Keywords: deep imaging; reflection-mode imaging; photoacoustic (PA) imaging; brain cortex; spleen.

Paper 07167LR received May 13, 2007; revised manuscript received Sep. 11, 2007; accepted for publication Sep. 12, 2007; published online Dec. 11, 2007.

Medical imaging has played an important role in exploring physiology and diagnosing disease. Optical imaging has the advantages of use of nonionizing radiation, low cost, optical contrast sensitive to physiological parameters, and access to various optical contrast agents. Owing to strong light scattering, however, purely optical imaging suffers from either shallow penetration or low resolution. Photoacoustic (PA) imaging, based on the detection of laser-induced internal acoustic waves, was designed to take advantage of optical absorption contrast yet achieve ultrasonic resolution. This technology can provide an imaging depth up to several centimeters in tissue.<sup>1</sup>

PA imaging can be implemented in the mode of either computed tomography or direct image formation. The former mode has been developed and employed to image the brain cortex and whole head of small animals and has provided high spatial resolution and low imaging artifacts.<sup>2,3</sup> This mode, however, has relatively poor out-of-plane (elevation) resolution. The latter mode is based on a focused ultrasonic transducer. In this mode, focusing provides transverse (lateral) resolution, whereas temporal resolution furnishes axial (depth) resolution.<sup>4</sup> Since bright-field illumination creates strong interference signals from tissue surfaces, Maslov et al. developed dark-field reflection-mode photoacoustic microscopy (PAM) to minimize the interference.<sup>5</sup> The initial implementation of PAM was based on a high-frequency (50-MHz) ultrasonic transducer providing high spatial resolution. However, the imaging depth was limited to  $\sim 3$  mm.

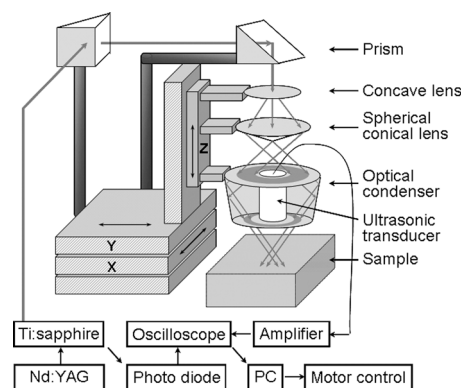


**Fig. 1** Schematic of the deep reflection-mode photoacoustic imaging system.

In this letter, as well as our conference report,<sup>6</sup> we present a scaled-up deep reflection-mode PA imaging system. The goal is to image much deeper than the 3-mm limit while the depth pixel count, defined as the ratio of the imaging depth to the axial resolution, is maintained at more than 100. The capability of deeper imaging enables noninvasive mapping of deep structures such as the spleen of relatively heavy, small animals.

The scaled-up reflection-mode PA imaging system is shown schematically in Fig. 1. The dark-field ring-shaped illumination is formed by a concave lens, a spherical conical lens, and an optical condenser in tandem. This illumination has a great advantage over bright-field illumination in that it can reduce the generation of surface PA waves and improve the detection of deep PA waves. The prisms mounted on an XY-linear translation stage enable higher optical energy delivery than the optical fibers used in the high-frequency PAM system.

To achieve deep penetration of light, we chose the 804-nm near-infrared wavelength for the excitation. This wavelength is an isosbestic point of the molar extinction spectra of oxy- and deoxy-hemoglobin. The light source is a tunable Ti:sapphire laser (LT-2211A, LOTIS TII) pumped by a Q-switched Nd:YAG laser (LS-2137/2, LOTIS TII). The laser system provides light pulses of a  $<15$ -ns pulse duration with a 10-Hz pulse repetition rate. The light beam is sufficiently broadened to conform to the maximum permissible exposure limit for the skin at this wavelength (31  $\text{mJ}/\text{cm}^2$ ).<sup>7</sup>

To receive deep PA signals with minimal ultrasonic attenuation, we chose a 5-MHz central frequency for the ultrasonic transducer (V308, Panametrics-NDT). This transducer is spherically focused with a 2.54-cm focal length, a 1.91-cm-diam active element, and a 72% nominal bandwidth. The use of a highly focused transducer (f-number: 1.33) is important for achieving good transverse resolution. The transducer is immersed in a water tank that has a 5 cm  $\times$  5 cm opening sealed with a thin clear membrane. A subject is scanned through this opening while acoustically coupled with acoustic gel (Ultrasound Scanning Gel, Sonotech, Inc.).

The PA signals are amplified by an amplifier (5072PR, Panametrics-NDT) and digitized and averaged by an oscilloscope (Tektronix TDS 5054). Signals from a photodiode

\*Tel: (314) 935-6152; E-mail: lhwang@biomed.wustl.edu

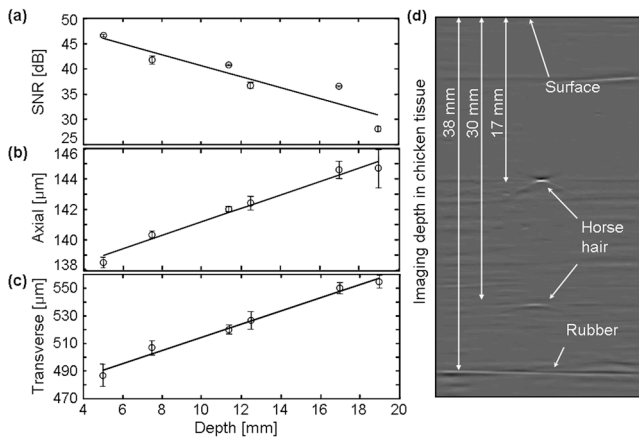


**Fig. 2** (a) SNR versus imaging depth (depth of the ultrasonic focal point). (b) Axial resolution versus imaging depth. (c) Transverse resolution versus imaging depth. (d) Demonstration of the maximum imaging depth ( $\sim 38$  mm) in chicken breast tissue.

(DET110, Thorlabs) are used to compensate for pulse-to-pulse fluctuations in laser energy. A computer controls the XY-linear translation stage for raster scanning and stores all the signals.

We estimated the peak-to-peak signal to root-mean-square noise ratio (SNR), axial resolution, and transverse resolution as a function of the imaging depth by imaging  $\sim 50\text{-}\mu\text{m}$ -diam human hair fibers [Figs. 2(a)–2(c)] in a 10% porcine gelatin containing 1% Lyposyn II. The reduced scattering coefficient ( $\mu_s'$ ) of this phantom<sup>8</sup> was  $\sim 10\text{ cm}^{-1}$ , which is close to that of biological tissues. At the 19-mm depth (the working distance of the transducer), images averaged 5 times achieved a  $\sim 28\text{-dB}$  SNR, a  $\sim 144\text{-}\mu\text{m}$  axial resolution, and a  $\sim 560\text{-}\mu\text{m}$  transverse resolution. The transverse resolution matches approximately the product of the f-number (1.33) and the central acoustic wavelength ( $\sim 421\text{ }\mu\text{m}$ , obtained from the PA signals). Therefore, the pixel count in the depth direction was 136, greater than the targeted 100. Compared with the resolution of micro-CT (20 to 100  $\mu\text{m}$ ) and micro-MRI (100 to 200  $\mu\text{m}$ ), the axial resolution of the proposed system is similar. However, the imaging depth is less than those of both CT and MRI. PA imaging, however, is sensitive to intrinsic functional optical contrast. Figure 2(d) demonstrates the possible maximum imaging depth in chicken breast tissue. We imaged two  $\sim 150\text{-}\mu\text{m}$ -diam horse hairs located  $\sim 17$  mm and  $\sim 30$  mm deep, where the SNRs were measured to be  $\sim 37$  dB and  $\sim 24$  dB, respectively, with 30 times averaging. Synthetic-aperture focusing and coherence weighting were applied to improve the transverse resolution as well as the SNR.<sup>9</sup> The rubber plate at a 38-mm depth was also imaged.

Internal organ imaging in both small and large animals is a valuable application of deep reflection-mode PA imaging. Internal organs such as the spleen have not been imaged reliably thus far using PA imaging techniques. Figure 3(a) shows the maximum amplitude projection (MAP) of the PA image of a spleen and a stomach of the rat weighing  $\sim 200$  g with the skin intact post mortem. Figure 3(b) shows the corresponding invasive anatomical photograph of the rat spleen obtained after PA imaging. The corresponding B-scan images in Fig. 3(c) show the depth information of the spleen and the stomach. The spleen was located  $\sim 2.0$  to 4.5 mm deep, and the adja-

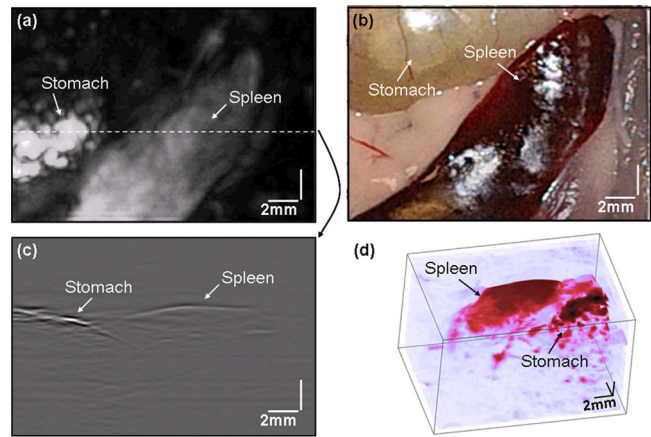


**Fig. 3** Noninvasive PA image of the spleen of a rat with the skin intact post mortem. (a) Noninvasive MAP image of the spleen and the stomach of the rat. (Color map was adjusted to show more details of the spleen by saturating the high intensity at the stomach.) (b) Corresponding invasive anatomical photograph. (c) B-scan image corresponding to the dashed line in (a) showing the depth information of the spleen and the stomach. (d) Three-dimensional (3-D) volumetric image showing the shape of the spleen and its depth.

cent stomach was even deeper. A three-dimensional (3-D) volumetric image is shown in Fig. 3(d), which reveals the contour of the spleen and its depth.

In summary, a deep reflection-mode 5-MHz PA imaging system was successfully constructed using dark-field illumination and a highly focused ultrasonic transducer. The imaging depth of this system was proven to be up to 38 mm in chicken breast tissue at the 804-nm wavelength. We imaged the spleen and the stomach of a rat, which have not been explored widely by PA imaging. In the future, continuous scanning and the use of a laser with a higher pulse repetition rate will be used to accelerate the data acquisition.

#### Acknowledgments

We are grateful to Konstantin Maslov and Xinmai Yang for experimental assistance. This research is sponsored in part by National Institutes of Health Grant Nos. R01 EB000712 and R01 NS46214 (BRP).

#### References

1. G. Ku and L. V. Wang, "Deeply penetrating photoacoustic tomography in biological tissues enhanced with an optical contrast agent," *Opt. Lett.* **30**, 507–509 (2005).
2. X. Wang, Y. Pang, G. Ku, X. Xie, G. Stoica, and L.-H. V. Wang, "Noninvasive laser-induced photoacoustic tomography for structural and functional *in vivo* imaging of the brain," *Nat. Biotechnol.* **21**, 803–806 (2003).
3. K. H. Song, G. Stoica, and L. V. Wang, "*In vivo* three-dimensional photoacoustic tomography of a whole mouse head," *Opt. Lett.* **31**, 2453–2455 (2006).
4. R. G. M. Kolkman, E. Honderbrink, W. Steenbergen, and F. F. M. de Mul, "*In vivo* photoacoustic imaging of blood vessels using an extreme-narrow aperture sensor," *IEEE J. Sel. Top. Quantum Electron.* **9**, 343–346 (2003).
5. K. Maslov, G. Stoica, and L.-H. V. Wang, "*In vivo* dark-field reflection-mode photoacoustic microscopy," *Opt. Lett.* **30**, 625–627 (2005).

6. K. H. Song and L. V. Wang, "Deep reflection-mode photoacoustic imaging and resolution scalability with depth," in *Proc. SPIE* 643773 (2007).
7. American National Standards Institute, "American National Standard for the safe use of lasers," ANSI Z136.1-2000, American National Standards Institute, New York (2000).
8. S. T. Flock, S. L. Jacques, B. C. Wilson, W. M. Star, and M. J. C. van Gemert, "Optical properties of Intralipid: A phantom medium for light propagation studies," *Lasers Surg. Med.* **12**, 510–519 (1992).
9. M.-L. Li, H. Zhang, K. Maslov, G. Stoica, and L.-H. Wang, "Improved *in vivo* photoacoustic microscopy based on a virtual detector concept," *Opt. Lett.* **31**, 474–476 (2006).